Journal of Achievements in Materials and Manufacturing Engineering
VOLUME 19
ISSUE 2
December
2006

Development of a mathematical model to study on variation of shielding gas in GTA welding

I.S. Kim [a,*], J.S. Son [a], H.J. Kim [b], B.A. Chin [c]
[a] Department of Mechanical Engineering, Mokpo National University, Jeonnam, 534-729, Korea
[b] Advanced Joining Technology Team, KITECH, Incheon, 406-130, Korea
[c] Department of Mechanical Engineering, Auburn University, AL, 36849-5341, USA
* Corresponding author: E-mail address: ilsookim@mokpo.ac.kr

Received in revised form 30.09.2006; accepted 31.10.2006

Analysis and modelling

ABSTRACT

Purpose: Generally discrete alternate supply of shielding gas is a new technology which alternately supplies the different kinds of shielding gases in weld zone. In this study, welding characteristics under variation of alternate supply method of shielding gases in austenite stainless steel using a GTA welding process have been investigated and found the relationship between different types of shielding gas and shielding gas supply.
Design/methodology/approach: 2-D axisymmetric heat and fluid mathematical model about weld pool has been developed for verifying the effect of alternate supply of shielding gas. The developed models were solved using a general thermofluid-mechanics computer program, PHOENICS code, which is based on SIMPLE algorithm.
Findings: The computed results showed that the developed computational models are very adequate to predict in the weld pool and bead geometry, and the technique of alternate supply of shielding gas should be useful to increase higher productivity, cost savings and better quality in arc welding.
Research limitations/implications: The effect of alternate supply of shielding gas should be useful to apply for a narrow-gap welding process.
Originality/value: The range of molten metal at the top of weld pool for supply of He shielding gas became wider than that for supply of Ar shielding gas. The developed computational models are very adequate to predict in the weld pool and bead geometry.
Keywords: Numerical techniques; Finite element method; GTA welding process; Shielding gas; Thermofluid-mechanics

1. Introduction

In general, GTA(Gas Tungsten Arc) welding is a welding method which has been used for many years to produce high quality joints in a swide variety of materials, while the process is sometimes called TIG (Tungsten Inert Gas-shield) welding by IIW(International Institute of Welding) [1]. The heat source is an electric arc between a tungsten electrode and a workpiece. The shielding gas which surrounds the electrode and the weld pool, forms an inert atmosphere which protects the electrode and the workpiece from atmosphere oxidation and favors the ignition and stability of the arc [2].

The extensive use of the GTA welding in industry applications has been limited due to the difficulty for choosing the optimal process parameters. Until now, only limited information on optimum welding conditions was available in the related literatures [3-23]. In case of thin plate square-butt configuration, the GTA welding process is usually run autogenously without the addition of filler metal. Furthermore, these conditions which required multi-pass welding and inter-pass grinding may be significantly important related to joint complete times. Thus, despite the high quality of joints produced by a conventional GTA welding, it does not find wide application in the fabrication of thicker materials due to its poor productivity.

In order to solve this problem, many attempts have been made to estimate the effect of process parameters experimentally.

Sosnin et al. [3,4] developed the experimental models for searching the optimum welding conditions of plasma welding with a penetrating arc. Gaillard et al. [5] proposed the methods for optimizing the preheat temperature to avoid the cracking of the resultant weld. Kikushima et al. [6] developed the system generating the optimal process parameter for the arc welding based on a heat conduction analysis. But for the above cases, an optimization technique was not used to determine the optimal process parameter. Ohji et al. [7] represented an algorithm for the control of optimal heat input, but mainly employed in GTA welding of plates. Ohji et al. [8-9] also applied for a computerized optimal control system of the GTA welding of thin plates based on the developed algorithm.

A alternate supply of shielding gas is a new technology that supplies the different kinds of shielding gases in weld zone discretely. Several researchers [24-28] reported a new technology capable of achieving better quality and high efficiency using the physical properties of welding arc which was produced by the periodical alternate supply of shielding gases in weld zone. Novikov et al. [24-26] suggested for the first time an advanced technology related to alternate supply of shielding gases in GMA(Gas Metal Arc) and GTA welding processes. They insisted that the defect incidence (porosity and crack) using alternate supply of Ar and He in 1420 and 1460 aluminum alloys have been decreased. Nsbarabokhin et al. [27] found the increased strength and improved ductility properties of welded joints of 1460 aluminum alloy has been carried out as alternate supply of Ar and He using the AC(alternate current) GTA welding machine. Yeo [28] has employed a low heat input by Ar shielding gas technique for first pass and a high heat input by He gas technique for second pass for joining the end plugs and cladding tube in order to avoid various types of weld defects, such as cracking, porosity, distortion. Furthermore, Nakamura et al. [29] reported a GMA welding process that periodically controls shielding gas composition, and a new welding torch that introduces locally and periodically CO_2 into Ar + 2%O_2 mixture to achieve high efficient welding were designed.

The purpose of this study is to investigate welding characteristics according to alternate supply of shielding gases in austenite stainless steel using a GTA welding process, and to find the variations in welding distortions and welding speed with different types of shielding gas and shielding gas supply. Finally, the comparison between the calculated and measured results has been carried out to verify the developed system. The part of information concerning at subject matter has been already presented in the paper [31].

2. Concept of the alternate supply of shielding gas

Compared to the method of the conventional gas supply in the GTA welding process, the new method of gas supply is alternately supplied in weld zone.

As shown in Fig. 1, in the case of alternate supply of Ar and He in constant arc length, the welding current increases and the arc voltage decreases. Conversely, as He is supplied into welding arc, the welding current decreases, and the arc voltage increases. This phenomenon results from the difference of the ionization potential between Ar and He. The effect from the variations of weld pool temperature gives proper weld penetration with heat input decreased. Meanwhile, when Ar and He were supplied, the welding current and arc pressure was periodically varied so that weld defect such as weld porosity, weld crack and lack of fusion was decreased.

This technology can realize better quality and high efficiency of weld employed variations in the physical properties of welding arc produced by the alternate supply of shielding gases as a simple and economical way. In practical use, it is difficult to study more systematic and better understand on this technology of alternate supply of shielding gases unlike conventional gas supply method. In addition, change of gas component, the increase of arc pressure following the periodic change of gas and arc pressure, the increase of fluidity of weld pool, the reduction of surface tension of molten metal and others are listed on the factors to make grain of weld zone refine. The combination of porosity, crevice and others is reduced and the density of welding part is increased significantly.

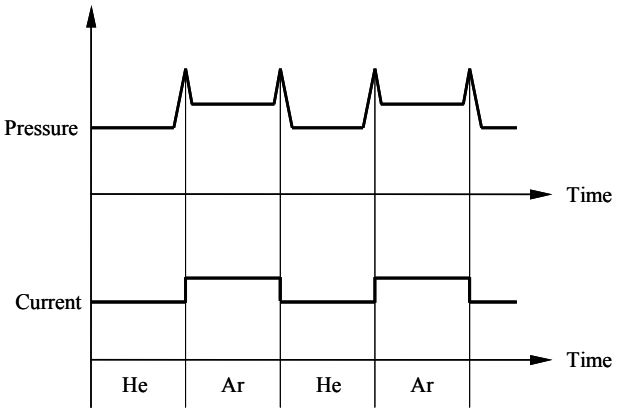

Fig. 1. Variation of pressure and current with alternate supply of shielding gas

Unlike the existing welding method that is constantly supplied with one type or mixed gas to use, the apparatus developed alternately supplies a discrete shielding gases with different flow rate. Apparatus for alternate supply of shielding gases is largely composed of two parts. One is the electronic part which controls the flow rate and supplies frequency of shielding gases, and the other is the valve that operated by electromagnetic force for alternate supply of shielding gases. The apparatus employed alternate supple of Ar gas and He gas. The impulse frequency and volume ratio is determined from the control part, adjusted it may adjust the volume ratio to 1:1~31:7 and the impulse frequency to 0:0~9:9 (2~10Hz) by operating the control lever. Once the input gas injected after setting, the frequency provides the electric signal to the coil of the impulse valve and the ratio of discharge provides the electric signal to the discharge control device. The gas penetrated into the accelerator moves into the impulse valve chamber and releases certain amount of the impulse pressure and discharge through the switch.

The supply of shielding gases in the case of alternate method is controlled by the electromagnetic valve. The sequence supply

of shielding gases was; when the valve is located on the left side, Ar or He is supplied. While the valve is located on the center, Ar and He is simultaneously supplied, and finally pure He or pure Ar is supplied as the valve is located on the right side.

In order to confirm a alternate supply of shielding gases developed in torch side, a doubt is created whether Ar and He is alternately supplied with given sequence in torch side or not because difference of density exists between Ar and He. Generally, on supplying Ar as shielding gas, welding current increases and arc voltage decrease, while on supplying He as shielding gas, welding current decreases and arc voltage increases. Also, the welding power source used in this study is of constant current type control and thus arc voltage waveforms were measured. Arc voltage waveforms by supplying Ar and He with respect to conventional method were compared with those by supplying Ar and He with alternate method. Fig. 2 shows arc voltage waveforms measured under different types of shielding gases and different combinations of shielding gases supply.

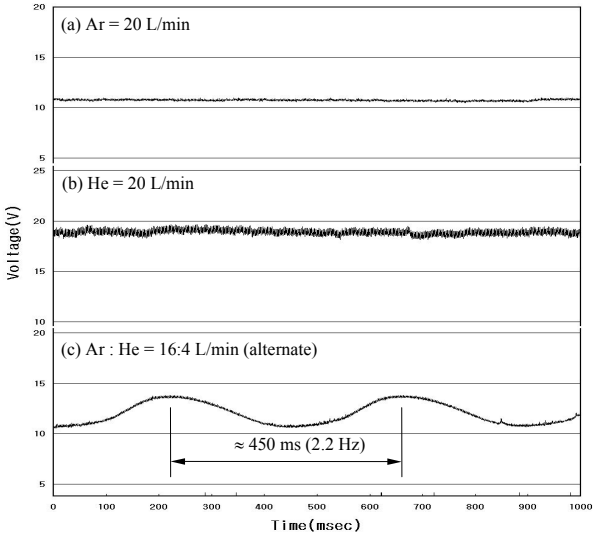

Fig. 2. Waveforms of arc voltage with types of gas and gas supply (100A, 15cm/min)

Figs. 2.(a) and 2.(b) were the arc voltage waveforms measured under a shielding gas atmosphere supplying Ar and He at a flow rate of 20L/min respectively by conventional method. The arc voltage waveforms measured under a shielding gas atmosphere supplying alternately Ar and He at flow rates of 14L/min. and 6L/min respectively by alternate method was shown in Fig. 2.(c). Compared with using Ar, the increase of arc voltage is about 8V in case of He. As shown in Fig. 2.(c), in case of supplying alternately Ar and He by alternate method under similar welding conditions as in Fig. 2.(a) arc voltage waveforms observed was the typical sine curve on which while supplying Ar as shielding gas, arc voltage decreased and while supplying He as shielding gas, arc voltage increased. However, in the arc voltage waveforms for alternate method, when compared with supplying He having a flow rate of 20L/min. as shown in Fig. 2.(b), arc voltage showed a lower value of about 5V. It can be concluded that when compared with the conventional method, the lower values observed in case of alternate method is measured due to use of lower flow rate, and apparatus used in the present study alternately supplies Ar and He with a frequency of about 2.2Hz. Fig. 3. shows the ratio of gas supply according to the frequency.

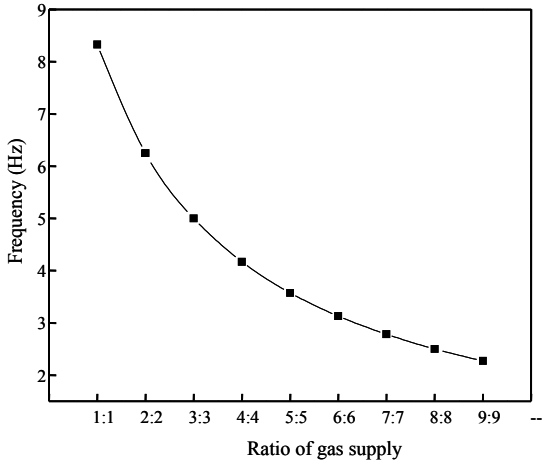

Fig. 3. Ratio of gas supply according to the frequency

3. Development of mathematical model

Fig. 4. is shown a schematic diagram of the GTA welding process. The flow of welding current from Anode (base metal) to Cathode (tungsten electrode) causes the self-induced magnetic field and plasma arc force as shown in Fig. 4. A plasma arc force acts as a distributed source of heat and electric current, impinges onto the base metal. This provides an incident flux of current and thermal energy at the free surface of the weld pool. The thermal energy generated in the arc causes the base metal to melt. Where the arc is maintained after the starting of arc, the supplied shielding gas is continuously ionized, and the ionized gas can be thought of as gaseous conductor, which allows the welding current to flow continuously. Mathematical model for weld pool has been developed to confirm the effect of alternate supply of shielding gas in the GTA welding.

In modeling system, the following assumptions wer made for analsys.

(1) The whole welding arc and weld pool model was axial symmetric.
(2) The arc plasma was in local thermodynamic equilibrium.
(3) Gas and metal liquid were incompressible.
(4) Arc plasma fluid were laminar.
(5) Surface of the weld pool is flat.
(6) Physical properties are constant except for the thermal conductivity, the specific heat and the density in the buyancy.
(7) The heat and current density distributions were obtained by the simulated results, which were calculated under the assumption of a steady state welding arc.
(8) Four distinct driving forces - Electromagnetic force caused by the interaction between the divergent current path in

the pool, Surface tension caused by temperature gradients at the weld pool surface and possibly by surface active agents in the weld pool, gas drag force caused by the impinging plasma jet, buoyancy force caused by the temperature gradient within the weld pool - were considered.

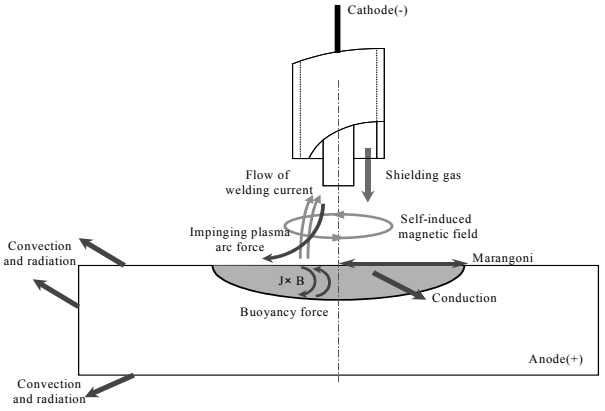

Fig. 4. A schematic diagram of the GTA welding process

3.1. Governing equations

The mass continuity equation is represented as:

$$\frac{1}{r}\frac{\partial}{\partial r}(\rho r u) + \frac{\partial}{\partial z}(\partial w) = 0 \tag{1}$$

The radial momentum equation is presented as:

$$\frac{\partial}{\partial t}(\rho u) + \frac{u}{r}\frac{\partial}{\partial r}(\rho r u) + w\frac{\partial}{\partial z}(\partial w) = \frac{2}{r}\frac{\partial}{\partial r}\left(\mu r \frac{\partial u}{\partial r}\right) + \frac{\partial}{\partial z}\left[\mu\left\{\frac{\partial w}{\partial r} + \frac{\partial u}{\partial z}\right\}\right] - \frac{\partial p}{\partial r} - 2\mu\frac{u}{r^2} - j_z B_\theta \tag{2}$$

The axial momentum equation is described as:

$$\frac{\partial}{\partial t}(\rho w) + \frac{u}{r}\frac{\partial}{\partial r}(\rho r w) + w\frac{\partial}{\partial z}(\partial w) = \frac{1}{r}\frac{\partial}{\partial r}\left[\mu r\left\{\frac{\partial u}{\partial z} + \frac{\partial w}{\partial r}\right\}\right] + 2\frac{\partial}{\partial z}\left(\mu\frac{\partial u}{\partial z}\right) - \frac{\partial p}{\partial r} - j_z B_\theta \tag{3}$$

The momentum equations consist of the transient term, two convective terms, pressure gradient term, the diffusive term and the Lorentz force term.

The energy equation can be expressed as:

$$\frac{\partial}{\partial t}(\rho C_p T) + \frac{u}{r}\frac{\partial}{\partial r}(\rho C_p r T) + w\frac{\partial}{\partial z}(\rho C_p T) = \frac{1}{r}\frac{\partial}{\partial r}\left(kr\frac{\partial T}{\partial r}\right) + \frac{\partial}{\partial z}\left(k\frac{\partial T}{\partial z}\right) - \frac{\Delta H}{C_p}\frac{\partial f_L}{\partial t} \tag{4}$$

The current continuity equation obtained from the definition of electric potential presented as:

$$\frac{1}{r}\frac{\partial}{\partial r}\left(\sigma r\frac{\partial \phi}{\partial r}\right) + \frac{\partial}{\partial z}\left(\sigma\frac{\partial \phi}{\partial z}\right) = 0 \tag{5}$$

The latent term is added to the conservation of thermal energy is can be expressed as:

$$\begin{aligned} f_L &= 1 && at \quad T > T_L \\ f_L &= \frac{T - T_S}{T_L - T_S} && at \quad T_S \le T \le T_L \\ f_L &= 0 && at \quad T > T_S \end{aligned} \tag{6}$$

Surface tension force, which is referred to as the Marangoni effect, describes the flow of liquid at a free surface from a region of low surface tension to a region of higher surface tension. At the surface of weld pools, the surface tension variation with temperature must be balanced by fluid shear stress since the surface must be continuous. Therefore, the shear stress at the surface is equated to the gradient of surface tension. At the free surface, the shear stress due to the surface tension driven flow is included as a boundary condition for the momentum equation.

$$\mu\frac{\partial V_S}{\partial z} = \frac{\partial \gamma}{\partial T}\frac{\partial T}{\partial s} \tag{7}$$

3.2. Boundary conditions

To complete the mathematical description of the problem, all of the boundary conditions are shown in Fig. 5. and Table 1. specified. The drag and the surface tension forces are treated as boundary conditions. The radial distribution of shear stress was employed. The liquid-solid phase change and the associated latent heat were modeled using the fixed grid method, which is the definition of the fraction of liquid. The essential feature of this method is that the evolution of latent heat is taken account of the governing energy equation by defining a heat source terms. Consequently, the numerical solution should be carry out on a space grid that remain fixed throughout the calculation.

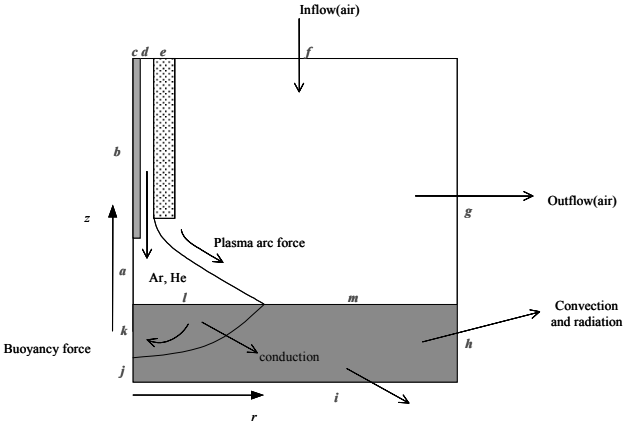

Fig. 5. A schematic diagram of boundary conditions for used a geometry model

In addition, The alternate supply of shielding gas ejected by the nozzle are simultaneously alternated with a different flow rate and frequency. The frequency of the alternated supply of shielding gas was included as shown the following equations [30], and performed with a uniform time step distribution.

$$T_T = \frac{Q_A T_A + Q_B T_B}{Q_T} \tag{8}$$

Table 1.
Boundary conditions for used geometry model

	u	w	T	ϕ
a	0	$\frac{\partial w}{\partial r}=0$	0	$\frac{\partial \phi}{\partial r}=0$
b, c	0	0	0	0
d	0	w_Q	$\frac{\partial T}{\partial r}=0$	ϕ
e, f	0	0	0	0
g	$\frac{\partial u}{\partial z}=0$	$\frac{\partial w}{\partial r}=0$	$\frac{\partial T}{\partial z}=0$	0
h	0	0	$h_c(T-T_\infty)=-k\frac{\partial T}{\partial z}$	0
i	0	0	$h_c(T-T_\infty)=-k\frac{\partial T}{\partial z}$	0
j	0	0	$\frac{\partial T}{\partial r}=0$	$\frac{\partial \phi}{\partial r}=0$
k	0	$\frac{\partial w}{\partial r}=0$	$\frac{\partial T}{\partial r}=0$	$\frac{\partial \phi}{\partial r}=0$
l	$-\mu\frac{\partial V_s}{\partial n}=\tau_{drag}+\frac{\partial \gamma}{\partial T}\frac{\partial T}{\partial s}$	0	$q_n(r)=-k\frac{\partial T}{\partial n}$	0
m	0	0	$q_n(r)=-k\frac{\partial T}{\partial n}$	0

3.3. Analysis method and procedure

In order to enhance the accuracy of calculation in weld pool area and to reduce the time of analysis, grid of variable spacing were employed. Fine grids were utilized near the current source at the welding arc model and the heat source at the weld pool model, while further away from it, a relatively coarse grid was employed. The mathematical models were employed a 50×12mm for weld pool non-uniform, fixed rectangular grid system for calculation of alternate supply of shielding gas. Magnitude of weld pool zone was estimated as approximated 10mm. Numerical calculations for weld pool were performed for the STS304 stainless steel plate. Table 2. shows the material properties for STS304 stainless steel taken from previous study [16], and the physical properties for shielding gas.

For a numerical solution of governing equations for developed mathematical model, the problem domain is covered by a set of rectangular volumes. Values of variables within a control volume are presented in term of the values at the associated node point. A main grid was located at the center of each control volume. The discretization was performed using a staggered grid, which consisted of two different grids; one for vector variables such as velocity and another for scalar variables such as temperature and pressure. Based on the staggered grid, a fully implicit control volume integration of the governing equations results in the finite difference scheme below:

$$A_P\phi_P = A_N\phi_N + A_S\phi_S + A_E\phi_E + A_W\phi_W + B \tag{9}$$

Table 2.
Material properties of STS304 stainless steel

Symbol	Nomenclature	Unit	Value
ρ	Density	kg/m^3	7200
μ	Effective viscosity	kg/m·s	0.05
σ	Electrical conductivity	1/Ω·m	7.7×10^5
ε	Emissivity of body surface	-	0.9
R	Gas constant	J/kg·mole·K	8314.3
ΔH	Latent heat of fusion	J/kg	2.47×10^5
T_L	Liquid temperature	K	1723
T_S	Solid temperature	K	1423
μ_0	Magnetic permeability of vacuum	H/m	1.26×10^{-6}

Where, ϕ presents any of axial and radial velocity, temperature, pressure and so on. The subscripts indicate the appropriate nodal value of dependent variable. The value of A represents the coefficients which results from the equations, but B is the source term from the equations, called discretization equations, were derived by integrating the governing differential equation over a each grid points.

To numerically solve the governing equations with the associated source terms, a general thermo-fluid mechanics computer program, PHOENICS code was employed. Convergence is completed when the spot values of temperature, pressure and velocities at the critical location remain uncharged(<0.1%) while the residuals of the governing equations continue to decrease. The residuals must generally decrease by at least 3 orders of magnitude with respect to the first sweep before the run is terminated. The time step used is 10^{-3} s. The number of sweeps needed material properties, fine turning of the relaxation parameters. The reference residual employed as a stopping criterion to determine when the calculations should advance to the next step, was assumed to be 10^{-9} for radial velocities, axial velocities, temperature and pressure.

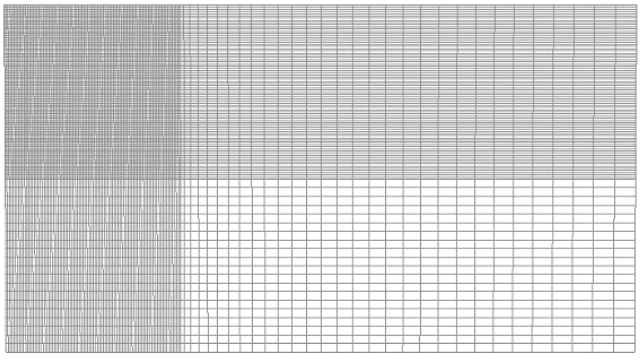

Fig. 6. Mesh generation employed in weld pool model

4. Numerical analysis results and discussions

4.1. Effect of alternate supply of shielding gas

In order to analyze the alternate supply of Ar and He shielding gas, additional input conditions were employed as shown in Table 3. For the alternate supply of shielding gas, supply of shielding was assumed to change at 0.3s Ar into the He. The simulations at 0.5s has been carried out.

Table 3.
Input conditions employed in simulation

Gas supply	Frequency (Hz)	Gas flow rate (L/min)	CTWD (mm)	Wire feed rate (m/min)	Welding voltage (V)	Arc current (A)
Ar:He	5:5	16:4	15	7.5	12	140

Fig. 7. shows the temperature distributions for alternate supply of shielding gas. When He supplied at the end of the supply of Ar shielding, range of heat transfer the welding arc become wider than Ar shielding, but the heat intensity at the weldment surface is deeper because of the different physical characteristics of Ar and He induced the arc intensity.

Fig. 8. represents the variations of arc pressure on the weldment surface for Ar and He. Arc pressure distributions on the weldment surface are similar the Gaussian distribution. When the distance from electrode tip center increased, the arc pressure decreased in different types of gas. But, arc pressure of Ar is higher than He about 3 times due to the different input gas flow rate and ionization potential of shielding gas. These results can be shown that the periodic change of gas and arc pressure will be increased fluidity of weld pool and the reduction of surface tension of molten metal.

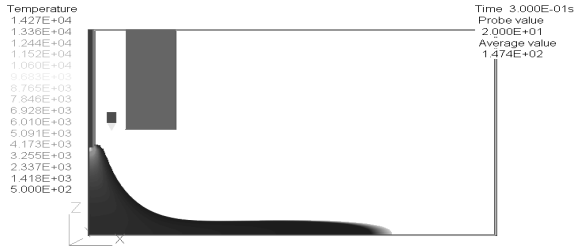

Fig. 7a. t = 0.30 sec

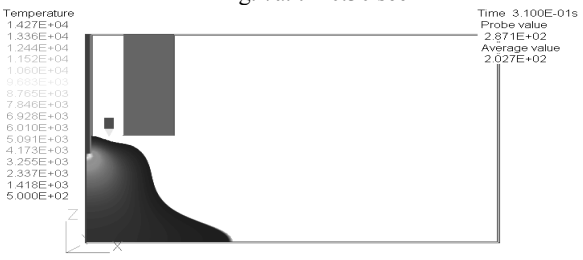

Fig. 7b. t = 0.31 sec

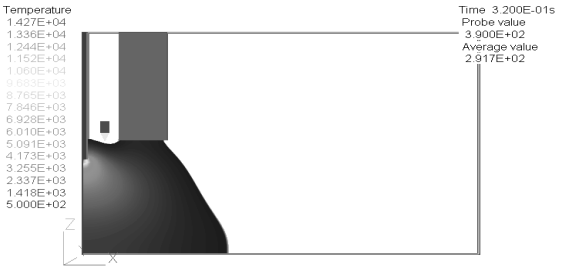

Fig. 7c. t = 0.32 sec

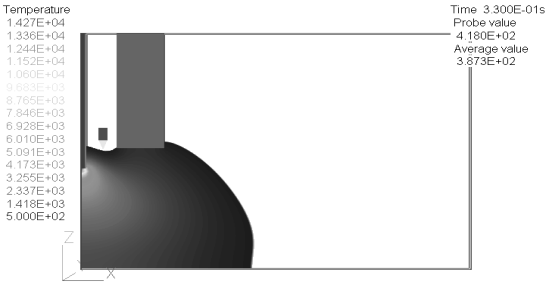

Fig. 7d. t = 0.33 sec

Fig. 7. Temperature distributions of Ar and He with alternate supply

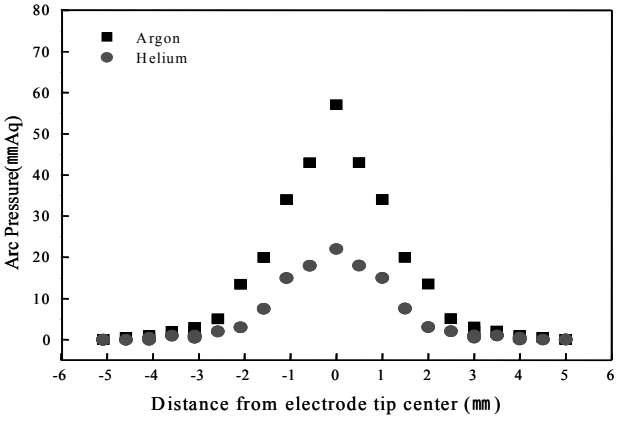

Fig. 8. The calculated results of the arc pressure on weldment surface for different types of shielding gas

4.2. Comparison of experimental and numerical results

The basic understanding of GTA welding process by a computational model requires the knowledge for the effect of various process parameters included type of shielding gas and interrelationship between process parameters and welding quality. In order to verify the developed mathematical models, the comparison between the calculated and measured results has been carried out. Experimental conditions were employed 200×100×12mm STS304 steel plates using the butt welding, and the types of gas and gas supply were chosen Ar+67%He and alternate supply of Ar and He as

a ratio of 5Hz. Welding input parameters for experiment and the simulation were employed in Table 3, and the experiments were carried out 4 times at each types of gas supply.

Fig. 9. shows comparison of the experimental and simulated results in a weld pool for the Ar+67%He shielding gas. According to Fig.6., the bead geometry for alternate supply of Ar and He has bigger bead width and deeper bead penetration. It can be illustrated from Fig.6 that the developed computational models are very adequate to predict in the weld pool and bead geometry.

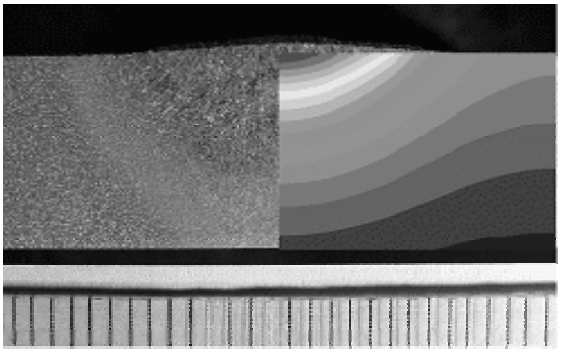

Fig. 9. Comparison of experimental and simulated results for Ar+67%He shielding gas

5. Conclusion and further studies

The experimental and a numerical research to find an interrelationship between alternate supply of shielding gas and weld quality in a GTA welding process has been carried out to check out the welding characteristics according to the variation of alternate supply of shielding gas. A two-dimensional axisymmetric heat and fluid mathematical models for a welding arc and weld pool was developed to verify the effect of alternate supply of shielding gas. The computed results showed that the range of molten metal at the top of weld pool for supply of He shielding gas became wider than that for supply of Ar shielding gas. However, the arc pressure of supply of Ar shielding gas was higher than that of He shielding gas about three times. The comparison between the calculated and measured results has been performed in order to verify the developed mathematical models The calculated bead width and bead penetration are in good agreement with the experimental results with about 5% relative error. These results showed that the developed computational models are very adequate to predict in the weld pool and bead geometry. It is also concluded that the effect of alternate supply of shielding gas should be useful to apply for a narrow -gap welding process.

References

[1] J. Cornu, Advanced Welding System 3(TIG and Related Processes), IFS, 1988.

[2] L.M. Gourd, Principle of Welding Technology, Edward Arnold, 1980.

[3] N.A. Sosin, Optimization of the Conditions of Plasma Welding with a Penetration Arc, Welding Journal 67 (1988) 311-314.

[4] V.V. Bashenko, N.A. Sosin, Optimization of the Plasma Arc Welding Process, Welding Journal 67 (1988) 233-237.

[5] R. Gaillard, S. Debiez, M. Hubert, J. Defourny, Methods for Optimizing the Preheat Temperature in Welding, Welding in the World 26 (1988) 230-249.

[6] S. Kikushima, R. Katsutani, Development of a Parameter Generating System for Arc Welding based on Heat Conduction Analysis, Welding International 9 (1987) 829-834.

[7] T. Ohji, K. Kondo, K. Nishiguchi, An Algorithm for Optimal Heat Input Control (1st Report), Q.J. of the Japan Welding Society 8 (1990) 48-52.

[8] T. Ohji, K. Kondo, K. Nishiguchi, M. Moriyasu, S. Hiramoto, W. Shimada, An Optimal Heat Input Control of Arc Welding (2nd Report), Q.J. of the Japan Welding Society, 8 (1990) 167-172.

[9] T. Ohji, Y. Kometani, Y. Yoshida, K. Nishiguchi, G. Tie, An Optimal Search of Arc Welding Parameters by a Numerical Model, Q.J. of the Japan Welding Society 8 (1990) 173-178.

[10] K.H. Tseng, C.P. Chou, The effect of pulsed GTA welding on the residual stress of a stainless steel weldment, Journal of Materials Processing Technology, 123 (2002) 346-353.

[11] L.R. Hwang, C.H. Gung, T.S. Shih, A study on the qualities of GTA-welded squeeze-cast A356 alloy, Journal of Materials Processing Technology 116 (2001) 101-113.

[12] H.G. Fan, Y.W. Shi, S.J. Na, Numerical analysis of the arc in pulsed current gas tungsten arc welding using a boundary-fitted coordinate, Journal of Materials Processing Technology 72 (1997) 437-445.

[13] C.M.D. Starling, P.V. Marques, P.J. Modenesi, Statistical modelling of narrow-gap GTA welding with magnetic arc oscillation, Journal of Materials Processing Technology 51 (1995) 37-49.

[14] A.H. ElSawy, Characterization of the GTAW fusion line phases for superferritic stainless steel weldments, Journal of Materials Processing Technology 118(2001) 127-131.

[15] A. Scotti, J.C. Dutra, V.A. Ferraresi, The influence of parameter settings on cathodic self-etching during aluminum welding, Journal of Materials Processing Technology 100 (2000) 179-187.

[16] J.I. Lee, K.W. Um, A prediction of welding process parameters by prediction of back-bead geometry, Journal of Materials Processing Technology 108 (2000) 106-113.

[17] A. Squillace, A.D. Fenzo, G. Giorleo, F. Bellucci, A comparison between FSW and TIG welding techniques: modifications of microstructure and pitting corrosion resistance in AA 2024-T3 butt joints, Journal of Materials Processing Technology 152 (2004) 97-105.

[18] G. Lothongkum, E. Viyanit, P. Bhandhubanyo1ng, Study on the effects of pulsed TIG welding parameters on delta-ferrite content, shape factor and bead quality in orbital welding of AISI 316L stainless steel plate, Journal of Materials Processing Technology 152 (2001) 233-238.

[19] G. Lothongkum, P. Chaumbai, P. Bhandhubanyong, TIG pulse welding of 304L austenitic stainless steel in flat, vertical and overhead positions, Journal of Materials Processing Technology 89 (1999) 410-414.

[20] S.C. Juang, Y.S. Tarng, H.R. Lii, A comparison between the back-propagation and counter-propagation networks in the modeling of the TIG welding process, Journal of Materials Processing Technology 75 (1998) 54-62.
[21] N. Murugan, V. Gunaraj, Prediction and control of weld bead geometry and shape relationships in submerged arc welding of pipes, Journal of Materials Processing Technology 168 (2005) 478-487.
[22] D.S. Nagesh, G.L. Datta, Prediction of weld bead geometry and penetration in shielded metal-arc welding using artificial neural networks, Journal of Materials Processing Technology 123 (2002) 303-312.
[23] M.A. Wahab, M.J. Painter M.H. Davies, The prediction of the temperature distribution and weld pool geometry in the gas metal arc welding process, Journal of Materials Processing Technology 77 (1998) 233-239.
[24] O.M. Novikov, Russian Patent No. 1808563, 1989.
[25] O.M. Novikov, Russian Patent No. 1816596, 1991.
[26] O.M. Novikov, Russian Patent No. 2008153, 1992.
[27] Nsbarabokhin, Y.U.G. Bushuev, E.V. Shulgina, V.A. Kazakov, O.N. Dudryashov, O.M. Novikov, N.V. Makarov, Technological Special Features of Welding 1460 High-Strenght Aluminium Alloy, Welding International 14 (2000) 468-470.
[28] D. Yeo, Apparatus and method for Producing Multi-Level Heat Input for Weld Formation using a Single Current Level Power Supply, U. S. Patent No. 4918287, 1990.
[29] N. Terumi, H. Kazuo, T. Makoto, S. Tomoaki, GMA Welding Process with Periodically Controlling Shielding Gas Composition, Q.J. of the Japan Welding Society 20 (2002) 237-245.
[30] D.B. Spalding, A Guide to PHOENICS Input Language-CHAM TR/100, CHAM, 1993.
[31] I.S. Kim, J.S. Son, H.J. Kim, B.A. Chin, A study on variation of shielding gas in GTA welding using finite element method, Worldwide Journal of Achievements in Materials and Manufacturing Vol. 17 (1-2), (2006) 249-252.